arXiv:1410.5735v2 [cond-mat.quant-gas] 25 Mar 2015

Nonequilibrium Phase Transition of Interacting Bosons in an Intra-Cavity Optical Lattice

M. Reza Bakhtiari[1], A. Hemmerich[2], H. Ritsch[3], and M. Thorwart[1]
[1] *I. Institut für Theoretische Physik, Universität Hamburg, Jungiusstraße 9, 20355 Hamburg, Germany*
[2] *Institut für Laser-Physik, Universität Hamburg, Luruper Chaussee 149, 22761 Hamburg, Germany*
[3] *Institute for Theoretical Physics, Universität Innsbruck, Technikerstraße 25, 6020 Innsbruck, Austria*

We investigate the nonlinear light-matter interaction of a Bose-Einstein condensate trapped in an external periodic potential inside an optical cavity, which is weakly coupled to the vacuum radiation modes and driven by a transverse pump field. Based on a generalized Bose-Hubbard model, which incorporates a single cavity mode, we include the collective back action of the atoms on the cavity light field and determine the nonequilibrium quantum phases within the non-perturbative bosonic dynamical mean-field theory. With the system parameters adapted to recent experiments, we find a quantum phase transition from a normal phase to a self-organized superfluid phase, which is related to the Hepp-Lieb-Dicke superradiance phase transition. For even stronger pumping, a self-organized Mott insulator phase arises.

PACS numbers: 32.80.-t, 42.50.Gy, 42.50.Pq, 42.50.Nn

High finesse optical cavities are nowadays routinely used in a wide range of fundamental and applied research [1] as a powerful tool to investigate the interaction of matter and light. Thus, the celebrated Jaynes Cummings (JC) model of a two-level atom coupled to a single mode of the radiation field [2] turned into a precise description of an experimental scenario that can be implemented in the laboratory [3]. Even more, modern optical cavities provide a tool to investigate *collective* matter-light interaction beyond a single-atom picture. An early insightful theoretical proposal [4] and a subsequent experiment [5] have shown that in a thermal atom ensemble in a high-finesse optical cavity, two different phases can emerge depending on the strength of an external pump laser field: a normal phase, characterized by a homogeneous density distribution and a vanishing intra-cavity field, and a self-organized (SO) phase, where the atoms form a matter grating trapped by a stationary intra-cavity optical standing wave. Only recently, similar experiments were realized with Bose-Einstein condensates (BECs) [6–8]. It was realized that in the limit of zero temperature and moderate external pumping this scenario represents an experimental implementation of the open Dicke model [9]. The normal-to-SO phase transition is directly related to the quantum phase transition early discovered in the Dicke model by Hepp and Lieb [10]. These results have triggered a tremendous revisit of the Dicke model [11].

An intriguing perspective is the extension of the present atom-cavity experiments to study lattice models with cavity mediated infinite range interactions. Experimentally this amounts to amending the BEC by an external periodic potential giving rise to an optical lattice. Depending on the choice of the spatial periodicity and phase of this additional lattice potential, very different physical scenarios can arise. A most natural choice is commensurability of the external lattice and the pump-induced lattice formed by photon scattering, such that a potential minimum of the pump-induced intra-cavity lattice potential corresponds to a minimum of the external lattice potential. However, conversely, not necessarily every minimum of the external potential coincides with a minimum of the intra-cavity lattice potential. In this case the pump-induced lattice acts to deepen every second minimum of the external lattice. This specific choice, studied in the present work, is compatible with the present experiments, and can be implemented by coupling laser beams of similar frequencies but different polarizations to the cavity as illustrated in Fig. 1.

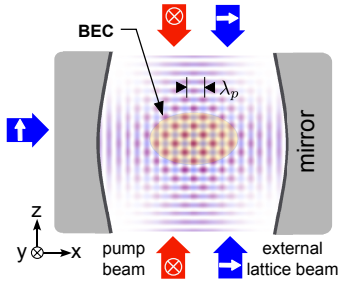

FIG. 1. Experimental setup. The external laser beams (blue) form a square lattice in the xz-plane with a lattice constant $\lambda_p/2$ (blue pattern). The linear polarization of the pump beams (red) along the y-direction allows scattering of photons into the cavity. This leads to a square lattice in the xz-plane rotated with respect to the external lattice by 45° with the lattice constant $\lambda_p/\sqrt{(2)}$ (red pattern). Each minimum of the pump-induced lattice potential coincides with a minimum of the external lattice potential. The wavelength of all beams is λ_p.

A comprehensive theory of the aforementioned physical scenario requires to combine two paradigmatic models. The Bose-Hubbard (BH) model has to be joined with the JC model to derive a generalized BH model [12–14] (hereafter, we follow Ref. [13]). Due to the strong interac-

tion of the atoms with the light field, the collective back action of the atoms on the light field is significant and the light field dynamics becomes strongly dependent on the dynamics of the atoms. In turn, the atomic dynamics is strongly driven by the light field and hence an inherent strongly non-linear collective dynamical behavior arises. An approach by treating the interatomic interaction in terms of an effective static mean field [15], which is very successful for the pure BH model [17], yields useful first insights. However, the collective interatomic interaction is an intrinsically time-dependent non-equilibrium quantity and hence a more refined treatment is necessary.

In this Letter, we use the bosonic dynamical mean field theory (BDMFT, see [18]) in which the quantum many-body interaction dynamically evolves and eventually can be evaluated self-consistently. Due to its non-perturbative nature, BDMFT is able to capture the strong dynamical back action induced by the cavity, as has been demonstrated in the pioneering work in Ref. [19]. An important scope of the present paper is to adapt BDMFT to model the realistic experimental scenario of Fig. 1 and present calculations of experimentally accessible observables versus the frequency and strength of the pump, which are the relevant tunable parameters in experiments. Our description of the pumped optical cavity includes the unavoidable cavity dissipation and the associated fluctuations due to the coupling to the bath of vacuum radiation modes. Below a critical pump we find a normal phase consisting of the conventional optical lattice formed by the external periodic potential, which remains unperturbed by pump photons scattered into the cavity in an uncorrelated manner. Above the critical pump, we find a SO phase, related to what has been observed in experiments without an external lattice. This SO phase is superfluid, i.e., both the SO and the superfluid order parameters are nonvanishing. At a second critical value of the pump strength, the system turns into a Mott insulator for even higher pump strengths. Our simulation results are compatible with a square root growth of the order parameter, (i.e. a critical exponent of 1/2) as function of the pump strength as also found in Refs. [15, 16]. We calculate the superfluid and SO order parameters, the depths of the associated effective intracavity optical potentials, the shape of the corresponding atomic density distributions, and study the dependence of the critical pump strengths on the values of the cavity decay rate and the pump-cavity detuning.

Generalized Bose-Hubbard model - We consider a BEC of N identical atoms of mass m trapped in an external periodic potential in the xz-plane with the motion along the y- direction assumed to be frozen out by a strong harmonic confinement with the harmonic frequency Ω given by $\hbar\Omega \approx 10\, E_{\rm rec}$ with $E_{\rm rec} \equiv \hbar^2 k^2/2m$ denoting the recoil energy, and $k = 2\pi/\lambda_p$. Hence, a description in terms of a conventional two-dimensional BH model with regard to the x and z coordinates is justified. This system is coupled to a standing wave cavity mode of frequency ω_c. The linear cavity is along the x-axis, characterized by a field decay rate κ, and pumped by a transverse optical standing wave along the z-direction with a strength V_p and the wavelength λ_p. Assuming the bad cavity limit $\hbar\,\kappa \gg E_{\rm rec}$, such that κ sets the fastest time scale [20], we may follow Ref. [13] and adiabatically eliminate the light field. By this, we may replace the photon field operator by a complex valued coherent field amplitude α, which is a function of the matter variables, and write the effective Hamiltonian [13, 19]

$$\mathcal{H} = -\sum_{\langle i,j\rangle} \tilde{J}_{ij}\, b_i^\dagger b_j + \frac{U}{2}\sum_i \hat{n}_i(\hat{n}_i - 1) \qquad (1)$$
$$+\, 2\,\mathrm{Re}(\alpha)\,\eta_{\rm eff}\,\tilde{J}_0 \sum_i (-1)^{i+1}\hat{n}_i + \sum_i (V_i^{\rm trap} - \mu_{\rm eff})\, b_i^\dagger b_i\,.$$

In passing, we note that the elimination of the light field is a very well-justified approximation for the setup of Ref. [6] but not for those of Refs. [7, 21], where the photons remain much longer inside the cavity before they are lost, such that an explicitly dynamical treatment of the light field is required. The first line in Eq. (1) exhibits a conventional BH Hamiltonian with bosonic annihilation (creation) operators for the atoms $b_i(b_i^\dagger)$, occupation number operators $\hat{n}_i = b_i^\dagger\, b_i$ at site i and the total particle number $N = \sum_i^{N_s} n_i$, where $N_s = n_L^2$ is the total number of sites in a $n_L \times n_L$ square lattice with the linear lattice size $L = n_L\lambda_p/2$. The nearest neighbor hopping amplitudes are $\tilde{J}_{ij} = \tilde{J}_x$ and $\tilde{J}_{ij} = \tilde{J}_z$ for hopping in the x- and z-direction, respectively, and U denotes the on-site collision energy per particle. A key element of $\mathcal{H}$ is the 3rd term with the effective pump laser strength $\eta_{\rm eff} = -\sqrt{|U_0|V_p}$, the light-shift per photon U_0, and $\alpha = \eta_{\rm eff}\tilde{J}_0 \sum_i (-1)^{i+1}\, n_i/(\Delta_c + i\kappa)$, where $\Delta_c = \omega_p - \omega_c - U_0 J_0 N$ denotes the effective pump-cavity detuning. The site-independent on-site matrix elements J_0 and $\tilde{J}_0$ associated with scattering photons within the cavity and between the pump and the cavity, respectively, follow after an expansion in terms of Wannier states. In the 4th term the effective chemical potential depends on the state of the light-field and reads $\mu_{\rm eff} = \mu_0 - U_0|\alpha|^2 J_0$. This directly expresses the interdependence between the state of the light field α and the chemical potential (i.e., the energy scale for adjusting the particle number), which is the origin of the nonlinear behavior of this system [12]. The fourth term also accounts for an additional external trapping potential shifting the energy of the site i by an amount $V_i^{\rm trap}$.

Unlike for the standard BH model, the hopping amplitudes $\tilde{J}_{x,z}$ and the on-site interaction U are not fixed *a priori*, but are given in terms of the instantaneous state of the photon field. In particular, in harmonic approximation one gets $\tilde{J}_{x,z} = \frac{4}{\sqrt{\pi}}(\frac{V_{x,z}}{E_{\rm rec}})^{3/4}\, \exp(-2\sqrt{V_{x,z}/E_{\rm rec}}\,)\, E_{\rm rec}$ and $U =$

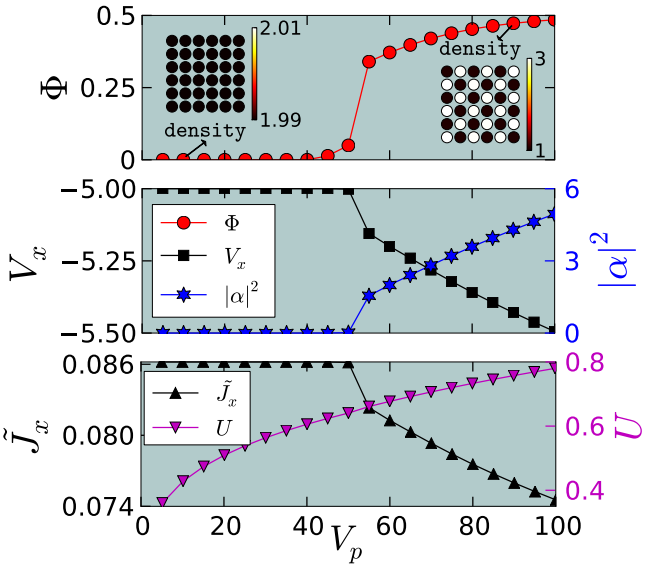

FIG. 2. Top: Order parameter Φ of the self-organized phase and two exemplary density distributions. Middle: Effective potential $V_{\rm eff} \equiv V_x = V_{\rm cl} + U_0|\alpha|^2$ along the cavity axis (left ordinate) and mean photon number $|\alpha|^2$ in the cavity (right ordinate). Bottom: Resulting hopping amplitude $\tilde{J}_x$ along the cavity (x) axis (left ordinate) and calculated on-site interaction U (right ordinate). All panels are vs the transverse pump laser strength V_p (in units of $E_{\rm rec}$). The cavity decay rate, detuning and external classical potential are $\kappa = 50\,E_{\rm rec}$, $\Delta_c = -2.8\,E_{\rm rec}$ and $V_{\rm cl} = -5\,E_{\rm rec}$.

$4\sqrt{2\pi}(\frac{a_s}{\lambda_p})\,(\frac{V_x V_z \hbar^2\Omega^2}{4E_{\rm rec}^4})^{1/4}\,E_{\rm rec}$ with $V_z = V_p$, $V_x = V_{\rm cl} + U_0\,|\alpha|^2$ and $V_{\rm cl}$ denoting the depth of the external lattice potential. The effective potential V_x along the cavity axis explicitly depends on the photon number, showing that the effective lattice potential inside the cavity is dynamically formed. For a realistic description, we set $V_{\rm ext} = -5\,E_{\rm rec}$ to ensure the validity of the tight-binding picture. We set the scattering length to $a_s = 5.77\,$nm and the pump laser wave length to $\lambda_p = 803\,$nm according to the setup in Refs. [7, 21]. In what follows, we focus on the homogeneous system and set the external trap potential to zero, i.e., $V_i^{\rm trap} = 0$. Moreover, we consider a given light shift of $U_0 = -0.1\,E_{\rm rec}$ at fixed temperature of $k_B T = 0.1\,E_{\rm rec}$. We have checked that this value of T is low enough to exclude any finite-temperature effect as discussed, e.g., in Ref. [22].

Method - To compute the resulting steady state of $\mathcal{H}$, we use BDMFT (see also Ref. [19]) which is analogous to the fermionic counterpart [23] and which is a nonperturbative approach to study a strongly correlated many-body bosonic system. The reliability of BDMFT depends on the behavior of the BH model in the limit of $z \to \infty$ where $z = 2d$ is the coordination number in a d-dimensional lattice [18]. In this limit, one can rigorously show that the BH model retains a local many-body self-energy. As a net result, the BH model is mapped onto an effective bosonic impurity model. Furthermore, a real-space extension of BDMFT has been developed recently which importantly incorporates any site-dependent behavior, either due to an external trapping potential [24, 25], or, solely by the underlying physics like the existence of a self-organized phase as in the current case. We eventually perform an exact diagonalization of the Anderson impurity model with fairly small numbers of orbitals ($n_s = 4-6$) to obtain the local densities n_i. Simultaneously, we monitor also the cavity photon number $|\alpha|^2$ until convergence for both parts is achieved. Throughout this work, we consider a fixed total particle number $N \simeq 72$ on a 6×6 lattice. Even though our main physical finding is captured sufficiently well with this lattice size, however finite size effect leads to minor modification of phase boundaries e.g in Fig. 4 . To quantify the self-organized quantum phase transition, we calculate the order parameter as [15, 19] $\Phi = \sum_i (-1)^i n_i / \sum_i n_i$. In a perfect conventional optical lattice with site-independent n_i, we get $\Phi = 0$, while for a perfect checkerboard density pattern with $n_i = \pm 1$, we have $\Phi = 1$.

Results - In the top panel of Fig. 2, we show the order parameter Φ of the self-organized phase vs. the transverse pump laser V_p. A clear quantum phase transition can be observed. A critical pump laser strength $V_p^{\rm crit}$ exists, below which the system is a conventional optical lattice with $n_i \simeq 2$. In other words, for $V_p < V_p^{\rm crit}$ the BEC atoms are homogeneously distributed across the potential minima of the external lattice, which exhibits square geometry with $\lambda_p/2$ separation of adjacent sites along the x- and z-directions, as is illustrated in the inset on the left-hand side of the upper panel. The scattering of pump photons into the cavity from atoms at adjacent lattice sites interferes destructively, such that the intra-cavity photon field α vanishes and the effective lattice depth V_x is thus given by the external lattice depth $V_{\rm cl} = -5\,E_{\rm rec}$, as is shown in the middle panel of Fig. 2. As is seen in the lowermost panel, the resulting hopping amplitude $\tilde{J}_x$ along the cavity axis is only determined by the external lattice and hence constant, while U grows monotonously due to the growing confinement in the z-direction resulting from the increasing intensity of the pump.

Upon increasing V_p, a pronounced quantum phase transition occurs. The BEC atoms, previously homogeneously distributed across all sites of the external lattice, self-organize to populate only every second site of the external lattice such that the Bragg condition for coherent scattering of pump light into the cavity is satisfied. Hence, a stationary intra-cavity field $|\alpha|$ emerges (see the middle panel in Fig. 2), which acts to deepen the potential wells at every second lattice site and thus stabilizes the self-organized density wave. The modulus of the associated effective potential V_x along the cavity axis increases (middle panel) and hence the atom hop-

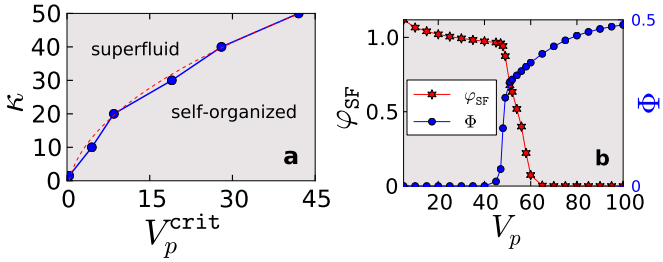

FIG. 3. (a) Phase boundary between the superfluid and the self-organized phase for varying cavity decay rates κ and critical pump laser strengths $V_p^{\rm crit}$ (both in units of $E_{\rm rec}$). The dashed line represents a square-root fit. (b) Superfluid order parameter $\varphi_{\rm SF}$ (left ordinate) and SO order parameter Φ (right ordinate) plotted against the pump strength V_p (in units of $E_{\rm rec}$). The cavity decay rate and the detuning are set to $\kappa = 50\,E_{\rm rec}$ and $\Delta_c = -2.8\,E_{\rm rec}$, respectively.

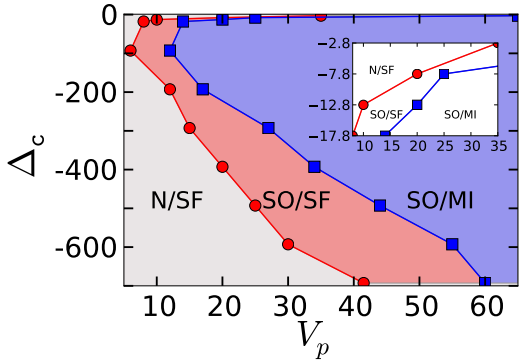

FIG. 4. Phase diagram with respect to Δ_c and V_p (both in units of $E_{\rm rec}$). N/SF refers to the normal superfluid phase, SO/SF to the self-organized superfluid phase and SO/MI to the self-organized Mott insulator. The inset shows a zoom of the main plot for small values of $|\Delta_c|$ ($\kappa = 50\,E_{\rm rec}$).

ping along the cavity axis $\tilde{J}_x$ is progressively impeded (lower panel). The order parameter Φ quantifying this self organization phenomenon (plotted in the top panel) acquires non-zero values. Note that the density modulation is between $n_i = 1$ and $n_i = 3$, such that we obtain $\Phi < 1$ even deeply within the SO phase. The corresponding real-space checkerboard-like density distribution is shown in the inset on the right-hand side. Depending on initial thermal or quantum fluctuations the SO density wave can arise with two spatial phases shifted with respect to each other by $\lambda_p/2$ along the x-axis, i.e., the system faces a symmetry breaking when crossing $V_p^{\rm crit}$. The SO phase transition also occurs for a vanishing depth of the external lattice, in which case it represents the well-known Dicke phase transition [2, 26] that has been observed in recent experiments [6, 7]. A related result for Φ vs V_p was obtained by a static mean-field approach [15], but we cannot quantitatively compare it with our results since in BDMFT the interactions are not fixed *a priori*, but are calculated dynamically and self-consistently. We note that in the regime of strong pumping, regions in the phase diagram have been identified within a strong coupling expansion where the phases show a finite compressibility [27].

In Fig. 3(a), we show the dependence of $V_p^{\rm crit}$ on κ and compare our calculations with a square-root fit as qualitatively suggested in Ref. [28]. Note that an increase of κ while U_0, and, hence the cavity finesse, is kept constant amounts to a decrease of the cavity length. The real-space BDMFT allows us also to calculate the superfluid order parameter $\varphi_{\rm SF} = \langle b \rangle$ [19]. This is depicted in Fig. 3(b) together with Φ. When Φ departs from zero at $V_p^{\rm crit}$, $\varphi_{\rm SF}$ begins to decrease. Interestingly, there is a sizable window in the vicinity of $V_p^{\rm crit}$ where $\varphi_{\rm SF}$ and Φ simultaneously coexist with a nonzero value, which is a manifestation of long-range superfluid order together with an SO density-wave. One may be tempted to call this state a supersolid phase [19, 29]. However, it should be noted that translational symmetry of the effective lattice, which traps the SO pattern, is not broken here because the lattice has an effective periodicity of λ corresponding to the density modulation of the atomic state. Above a certain value of V_p, $\varphi_{\rm SF}$ vanishes, and the Mott insulating phase arises.

In Fig. 4, we depict the phase diagram of our system with respect to V_p and negative pump-cavity detuning $\Delta_c < 0$ for a fixed cavity decay rate $\kappa = 50\,E_{\rm rec}$. The phase boundary between the normal phase and the self-organized superfluid phase (SO/SF) is found in accordance with the experiments in Refs. [6, 8]. For small $|\Delta_c| < 100\,E_{\rm rec}$ (see inset), the critical pump power scales inversely with $|\Delta_c|$ while for large values of $|\Delta_c|$, it scales linearly with $|\Delta_c|$. The notable increase of $V_p^{\rm crit}$ as $|\Delta_c|$ falls below κ is explained as follows: the intra-cavity field is driven by the pump field with a phase delay approaching $\pi/2$ as Δ_c approaches zero and hence the two fields cease to interfere. Hence, the resulting light field acquires potential minima of equal depth at each potential minimum of the external potential. The checkerboard density wave pattern is then no longer supported and hence the scattering of light into the cavity is suppressed. Note that a similar phase boundary is found for large atom samples with no external lattice described by a semi-classical kinetic Vlasov equation which neglects all correlations [16]. Even though our particle number is much smaller than in Ref. [16], we still correctly capture the qualitative mean field physics. A second phase boundary occurs, where the self-organized phase becomes a Mott insulator (SO/MI).

In conclusion, we have solved the generalized Bose-Hubbard model for an optical lattice of bosons interacting collectively with an optical cavity mode in a scenario adapted to recent experiments. Using the non-perturbative real-space BDMFT, we find two nonequilibrium quantum phase transitions upon increasing the

strength of a transverse pump field. A quantum phase transition from the normal phase to a self-organized superfluid phase occurs. For even stronger pumping, a pure self-organized Mott insulator phase arises.

This work was supported by the SFB925 (projects C5 and C8) and by the Austrian Science Fund project S4013. We acknowledge useful discussions with M. Wolke, H. Kessler, J. Klinder, J. Larson, P. Nalbach, L. He and Y. Li. In particular, M.R.B. thanks Walter Hofstetter for his previous major input on the familiarization with DMFT.

[1] K. Vahala, Nature **424**, 839 (2003).
[2] G. Agarwal, *Quantum Optics* (Cambridge University Press, 2012).
[3] S. Haroche and J.-M. Raimond, *Exploring the Quantum* (Oxford University Press, 2006).
[4] P. Domokos and H. Ritsch, Phys. Rev. Lett. **89**, 253003 (2002).
[5] A. T. Black, H. W. Chan, and V. Vuletic, Phys. Rev. Lett. **91**, 203001 (2003).
[6] K. Baumann, C. Guerlin, F. Brennecke, and T. Esslinger, Nature **464**, 1301 (2010).
[7] H. Keßler, J. Klinder, M. Wolke, and A. Hemmerich, Phys. Rev. Lett. **113**, 070404 (2014).
[8] J. Klinder, H. Keßler, M. Wolke, L. Mathey, A. Hemmerich, Proc. Natl. Acad. Sci. USA **112**, 3290 (2015).
[9] R. H. Dicke, Phys. Rev. **93**, 99 (1954).
[10] K. Hepp and E. H. Lieb, Ann. Phys. **76**, 360-404 (1973).
[11] H. Ritsch, P. Domokos, F. Brennecke, and T. Esslinger, Rev. Mod. Phys. **85**, 553 (2013).
[12] C. Maschler and H. Ritsch, Phys. Rev. Lett. **95**, 260401 (2005).
[13] C. Maschler, I. B. Mekhov, and H. Ritsch, Eur. Phys. J. D **46**, 545 (2008).
[14] J. Larson, B. Damski, G. Morigi, and M. Lewenstein, Phys. Rev. Lett. **100**, 050401 (2008).
[15] D. Nagy, G. Szirmai, and P. Domokos, Eur. Phys. J. D **48**, 127 (2008).
[16] W. Niedenzu, T. Griesser and H. Ritsch, EPL **96**, 43001 (2011).
[17] M. Lewenstein, A. Sanpera, and V. Ahufinger, *Ultracold Atoms in Optical Lattices: Simulating quantum many-body systems* (Oxford University Press, 2012).
[18] M. Snoek and W. Hofstetter, in *Quantum Gases: Finite Temperature and Non-Equilibrium Dynamics*, edited by M.D.N.P. Proukakis, S.A. Gardiner and M. Szymanska (Imperial College Press, 2013), arXiv:1007.5223.
[19] Y. Li, L. He, and W. Hofstetter, Phys. Rev. A **87**, 051604 (2013).
[20] C. Gardiner and P. Zoller, *The Quantum World of Ultra-Cold Atoms and Light: Book 1: Foundations of Quantum Optics* (Imperial College Press, 2014).
[21] M. Wolke, J. Klinner, H. Keßler, and A. Hemmerich, Science **337**, 75 (2012).
[22] F. Piazza, P. Strack, W. Zwerger, Annals of Physics **339**, 135 (2013).
[23] D. Vollhardt, Ann. Phys. (Berlin) **524**, 1 (2012).
[24] Y. Li, M. R. Bakhtiari, L. He, and W. Hofstetter, Phys. Rev. B **84**, 144411 (2011).
[25] Y. Li, M. R. Bakhtiari, L. He, and W. Hofstetter, Phys. Rev. A **85**, 023624 (2012).
[26] M. Gross and S. Haroche, Phys. Rep. **93**, 301 (1982).
[27] S. Fernández-Vidal, G. De Chiara, J. Larson, and G. Morigi, Phys. Rev. A **81**, 043407 (2010).
[28] M. Kulkarni, B. Öztop, and H. E. Türeci, Phys. Rev. Lett. **111**, 220408 (2013).
[29] M. Boninsegni and N. V. Prokof'ev, Rev. Mod. Phys. **84**, 759 (2012).